Journal of King Saud University – Science 32 (2020) 3230–3236

Contents lists available at ScienceDirect

Journal of King Saud University – Science

journal homepage: www.sciencedirect.com

Original article

Dexmedetomidine improves anesthesia of complicated congenital heart disease in infants based on improved magnetic resonance imaging

Xiaoyan Xu, Jianzhong Shuai, Fenlan Xu, Zhenhua Huang, Cheng Zhang *

Department of Anesthesia, Chengdu Women's & Children's Central Hospital, Chengdu 610000, China

ARTICLE INFO

Article history:
Received 19 January 2020
Revised 26 February 2020
Accepted 28 March 2020
Available online 1 April 2020

Keywords:
Improved MRI images
Dexmedetomidine
Infants
Complex congenital surgery

ABSTRACT

Dexmedetomidine is a very useful anesthetic, and it currently has less improvement in early childhood surgery. In order to study the effect of dexmedetomidine in improving the complex congenital heart surgery in infants and young children, this paper used machine learning algorithm to improve the image, and combined MRI (Magnetic Resonance Imaging) images for diagnostic analysis. At the same time, this paper collected experimental data to carry out algorithm analysis, collected cases to design experiments, used the method proposed in this paper to conduct research, and recorded the research results. Through comparative analysis, the algorithm proposed in this study has certain effects. Moreover, it has been proved that the dexmedetomidine infants have complicated effects in complex anesthesia surgery and can provide theoretical reference for subsequent related research.

1. Introduction

In recent years, research reports have found that this product also has anti-sympathetic properties, maintains hemodynamic stability and reduces the dose of general anesthesia. Moreover, it has been widely used in clinical practice and has achieved good anesthetic effects. Recent studies have shown that dexmedetomidine is a clinically valuable alternative to midazolam sedation and increases the comfort of clinical procedures (Ahmad et al., 2017) and reduces the risk of postoperative mechanical ventilation sedation (Alhammad et al., 2017).

Dexmedetomidine is used as a preoperative medication and can be used in children. Moreover, whether administered orally or intranasally, it provides a satisfactory level of sedation, facilitates parental separation, and makes the child easy to receive a mask (Ama and Yassin, 2017), and can also alleviate the sevoflurane anesthesia during the recovery period (Amorim et al., 2017). However, for oral or intranasal administration of dexmedetomidine, which administration method is superior requires more research. In addition, when it is used for preoperative intravenous administration in adults, dexmedetomidine can reduce intraocular pressure during induction of general anesthesia and reduce intubation pressor response (Chen et al., 2018).

Dexmedetomidine has the characteristics of improving the pharmacological properties of peripheral and intra-spinal local anesthesia, and is currently the most potential adjuvant drug (Schäffer and Otero, 2017). However, there have been many preclinical and clinical studies showing that it is safe and effective for clinical practice. The highly lipophilic dexmedetomidine is rapidly absorbed into the cerebrospinal fluid and binds to the spinal cord alpha 2 receptor to produce an analgesic effect. Numerous studies have shown that dexmedetomidine combined with local anesthetics can prolong the duration of sensory block, motor block and analgesia (Frölich et al., 2017) and reduce the onset of sensory block and motor block in spinal anesthesia. In addition, for spinal anesthesia, dexmedetomidine combined with local anesthetics or intravenous infusion of dexmedetomidine can prolong the duration of sensory block, motor block and analgesia (Hussain et al., 2017).

The high incidence of cardiovascular accidents and other complications during perioperative cardiac surgery can lead to increased patient mortality and prolonged hospital stay. However, the use of perioperative dexmedetomidine may be beneficial for the clinical outcome of cardiac surgery. A meta-analysis showed that dexmedetomidine for perioperative cardiac surgery not only reduced the risk of postoperative ventricular tachycardia and sputum and atrial fibrillation, but also shortened ICU stay time and

* Corresponding author.
E-mail address: z4ang.cheng@yandex.com (C. Zhang).
Peer review under responsibility of King Saud University.

Production and hosting by Elsevier

https://doi.org/10.1016/j.jksus.2020.03.043
1018-3647/

hospital stay. However, it may increase the risk of bradycardia and hypotension (Jia et al., 2017). In addition, dexmedetomidine can reduce the incidence of acute renal failure after cardiac surgery (Jian-Xin et al., 2017). In addition to inhibiting hemodynamic responses during endotracheal intubation, dexmedetomidine also reduces the severity of myocardial ischemia during cardiac surgery and protects the myocardium. Although dexmedetomidine has some side effects, it is an effective adjuvant that can be safely and effectively used in heart surgery.

The application of dexmedetomidine is of great value for neurosurgery. Jo et al. (2017) compared dexmedetomidine sedation techniques and general anesthesia for chronic subdural hematoma surgery found that the combination of dexmedetomidine sedation and local anesthesia has a short operation time, low hemodynamic fluctuation, less postoperative complications, short hospital stay, and is a safe and effective technique for drilling and drainage of chronic subdural hematoma. In addition to providing cerebral hemodynamic stability (Khare et al., 2017), this product can also prevent sudden increase of intracranial pressure during insertion, extubation and insertion of skull nails. At the same time, dexmedetomidine has a certain effect on the occurrence of neurosurgery. Küçükebe et al. (2017) retrospectively evaluated the efficacy of dexmedetomidine in 72 patients with paroxysmal sympathetic hyperactivity (PSH) after neurosurgery and found that compared with propofol, dexmedetomidine can effectively control the acute exacerbation of PSH, but it cannot improve the long-term prognosis of patients. As an adjuvant for postoperative analgesia, Su et al reported that dexmedetomidine 0.02 μg/kg/h + sufentanil 0.02 μg/kg/h can reduce the number of opioids after neurosurgery, reduce the incidence of adverse reactions, and improve pain score.

Although dexmedetomidine has not been approved by the FDA for pediatric patients, clinical studies have shown that it can be effectively used for sedation in clinical pediatric patients. A meta-analysis showed that compared with other drugs, intranasal administration of dexmedetomidine prior to surgery provides more satisfactory sedation, is prone to separation from parents, and reduces the incidence of analgesics and nasal irritation and postoperative nausea and vomiting.

2. Research method

2.1. Convolutional neural network algorithm

The application of dexmedetomidine is of great value for neurosurgery. Jo et al. (2017) compared dexmedetomidine sedation techniques and general anesthesia for chronic subdural hematoma surgery found that the combination of dexmedetomidine sedation and local anesthesia has a short operation time, low hemodynamic fluctuation, less postoperative complications, short hospital stay, and is a safe and effective technique for drilling and drainage of chronic subdural hematoma. Compared with other drugs, this study has inherent advantages, so dexmedetomidine was selected.

The composition of a convolutional neural network is relatively simple. It consists of an input layer, a convolutional layer, a pooling layer, a fully connected layer, and an output layer. In order to construct a deeper convolutional neural network, the convolutional layer and the pooling layer will appear multiple times. The convolutional layer and the pooling layer appear alternately. There is a convolutional layer and then a pooling layer. Appears many times. It shows high recognition accuracy in image recognition, and has good performance and low memory consumption. Therefore, in this study, a convolutional neural network was selected as the image recognition algorithm.

The convolutional neural network algorithm is mainly divided into two processes. The first part is the forward propagation algorithm. The input data is transmitted through the network structure to obtain the output, and the residual value of the cost function is obtained. The second part is derived from the cost function, and the backpropagation modifies the parameters. After that, the two processes are repeated continuously, and the residuals with the tags are continuously reduced until the residuals are reduced to a stable state, and the network parameters are stable (Li and Liu, 2017).

At the time of data transfer, the actual data is a four-dimensional array blob, as shown in Fig. 1, which is the number of pictures N, the number of channels K, the height H of the image, and the width W of the image. The number of pictures N is the number of pictures in the smallest batch. After N pictures, the LOSS is calculated once and then passed back. For the input layer, the number of channels in the grayscale image is 1, and the channel in the color map is 3, but for a layer in the middle, the number of channels is the current number of feature maps. H, W refers to the height and width of the image. If it is a convolution kernel, it represents the size of the convolution. In order to ensure the symmetry transfer, H and W are equal. The small square in Fig. 1 is the storage unit for the data. Because the data transfer in a convolutional neural network has both forward and reverse passes, its value must contain two parts, the normal value of the forward transfer, and the derivative value of the reverse pass. Different layers are formed based on the Blob module, and different layers are combined with each other to form a network (Makhni et al., 2017).

Each convolutional neural network is composed of basic layers, as shown in Fig. 2, and the input to these layers is the data unit Blob, and the output is also a Blob. However, the types or numbers of layers included in different networks are different, and the results achieved are quite different.

2.2. Hierarchical structure of convolutional neural networks

2.2.1. Input layer

The input layer is the input port of the convolutional neural network, which inputs the original image into the network. For convolutional neural networks with supervised learning, the input contains the Data, and the corresponding Label (Messeha and El-Morsy, 2018).

2.2.2. Convolution layer

The convolution layer connects the parts of the input image and calculates the feature maps associated with the specific convolution kernel. The resulting output feature map size is 3×3. The size of the output value is expressed as (Messeha and El-Morsy, 2018) (Fig. 3):

$$Y_i = \sum_{i=1}^{k} \sum_{j=1}^{k} X_{ij} \times W_{ij} + b \tag{1}$$

If Padding is added, the convolution process is shown in Fig. 4. The added Padding is 1, that is, a white edge with zero data is added around the outermost edge of the image If other parameters are inconvenient, the initial convolution position of the convolution becomes the position in the graph. The output size will also be changed accordingly. The relational expression for the size of the output feature map and the size of the convolution kernel, the step size, the size of Padding, etc. is as in (Miller et al., 2018):

$$N_{out} = \frac{N_{in} - k + 2P}{S} + 1 \tag{2}$$

2.2.3. Pooling layer

The Pooling Layer, the down-sampling layer, can reduce the size of the input image and reduce the number of features, which can speed up the training. More importantly, the main information of

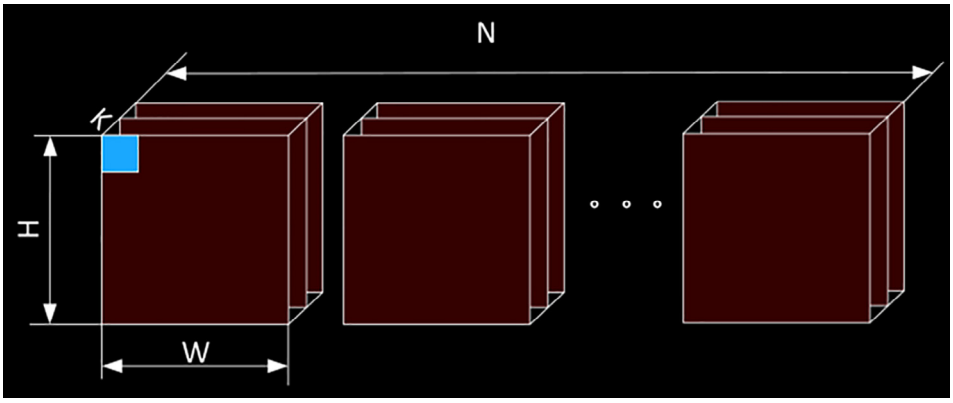

Fig. 1. Schematic diagram of the data storage unit.

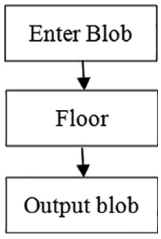

Fig. 2. Connection diagram between data storage unit Blob and layer.

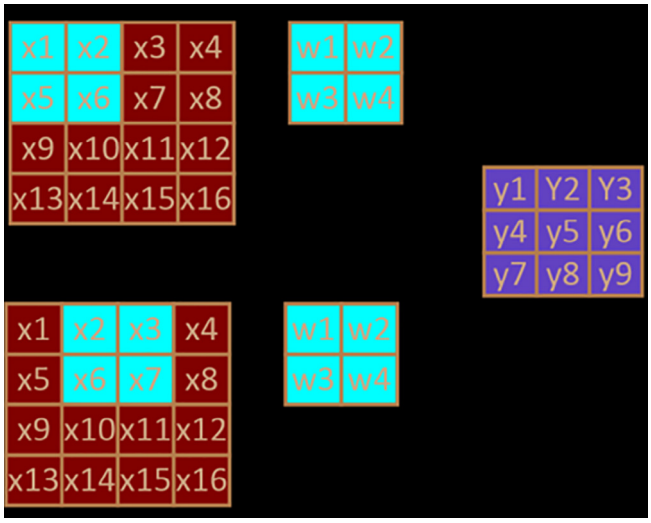

Fig. 3. Schematic diagram of convolution without Padding.

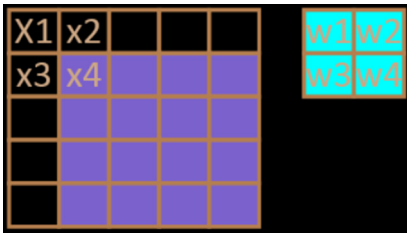

Fig. 4. Schematic diagram of convolution with Padding.

the window is extracted, which not only satisfies the reduction of the data dimension, but also retains important information. It is often followed by a convolutional layer, the window size is also, and the step size is 2. There are three common ways, namely, Average Pooling, Max Pooling, and Stochastic-pooling.

For the average pooling, as shown in Fig. 5(a), the forward values are averaged, and the corresponding expression is (Mohamed et al., 2018):

$$X_{out} = \frac{\sum_{i=1}^{k\times k} X_i}{k \times k} \tag{3}$$

Among them, X_{out} is the output of the Polling layer, X_i is the output of the Pooling layer, k is the window size for down-sampling, and the default step size is the same as the window.

As shown in Fig. 6(a), when passing in the reverse direction, the value of diff in the blob is used to directly divide the input value by the square of the window size k. The value corresponding to each window is the same, as shown

$$X_{out} = \frac{X_i}{k \times k} \tag{4}$$

In the case of forward propagation, only the maximum value of the data corresponding to the window is taken as the final result. That is, the expression is (Shen et al., 2017):

$$X_{out} = \max_{0\leqslant i\leqslant k\times k} X_i \tag{5}$$

When the reverse is transmitted, as shown in Fig. 6(b), the maximum value is filled in the original position, and the other values are 0.

2.2.4. Activation layer

For the activation layer, the mathematical essence is to transform the linear relationship of data into a nonlinear relationship, which will transform its dimension into a high-dimensional space, so that the latter can find different features in different dimensions. Its network characteristics emulates biological neurotransmission. The vast neural network system works only 10% to 20%, and other neurons are inactive. Only when the characteristics of the training set and the activation function correspond to each other, a better network structure and network training effect can be obtained. There are also some activation functions and activation layers, which are improved based on the RELU activation function. At the same time, the number of parameters is increased, and the training time is increased (Yoo et al., 2017).

2.2.5. Dropout layer

The Dropout layer is similar to our activation function, except that the Dropout layer only works in backpropagation. When backpropagation, some nodes are activated, some nodes are not activated, and it is a layer that discards the partial discard connection.

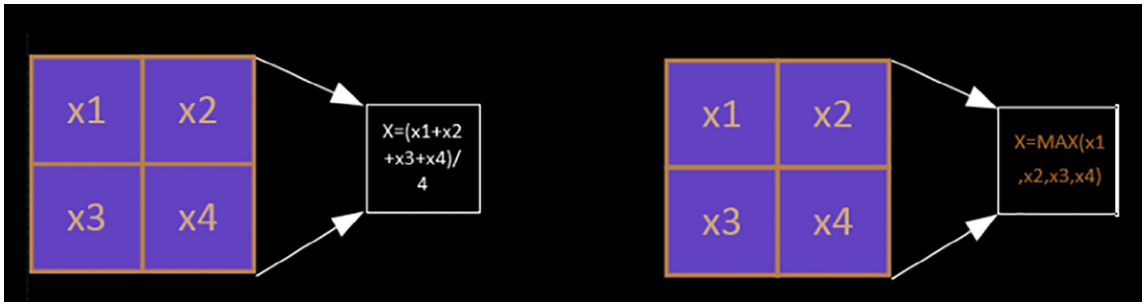

Fig. 5. Pooled layer forward propagation.

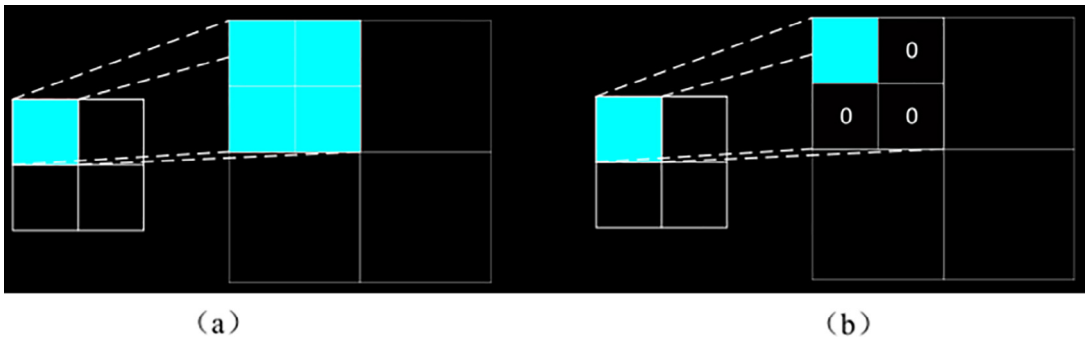

Fig. 6. Pooled layer back propagation.

2.2.6. Fully connected layer

The feature map is output by the convolutional layer or the down-sampling layer, which is generally a square matrix of MXM. It is expanded in rows into a one-dimensional column vector, and each point on the feature vector is connected to each point of the output vector. Each line represents a weight, then the weight of the fully connected layer is a matrix of TXNs. For example, handwriting recognition, whose output is 10 categories, then T is 10, and if it is a white cell three classification, it is 3.

2.2.7. Decision layer

The decision layer is mainly based on the extracted features of the convolution layer, the down-sampling layer, the active layer, and the fully connected layer of the previous stage, and outputs the input type of the input graph to determine which class the input belongs to.

The formula of the Softmax function is shown in Eq. (6).

$$S_j = e^{\alpha_j} / \sum_{k=1}^{T} e^{\alpha_k} \tag{6}$$

Fig. 7. Cardiac MRI image.

Among them, j is the output vector index and T is the dimension of the output vector. k is the probability vector that converts the input vector into a group. The type corresponding to the largest probability value is the output type.

2.2.8. Loss layer

However, in training, a deviation is obtained, which measures the deviation of the input from the convolutional neural network output from its actual label. The function for calculating this deviation is called the loss function. In fact, this loss function is a multivariate function containing the parameters of the ownership value W and the offset b variable. In order to minimize the output of this function, the derivative is reverse-transferred, and W and b are modified to make the function take the minimum value. Currently, different networks use different loss functions, such as Softmax With Loss, Euclidean Loss, Hinge Loss, and so on.

The mathematical expression for the reverse derivative transfer is:

$$\frac{d}{dx}f_{(g(x))} = f'_{(g(x))}g'(x) \tag{7}$$

However, the Loss function is a multivariate function. When one of the variables is valued, it needs to find the partial derivative, and the above formula is converted into

$$\frac{\partial}{\partial W_i}L_{(W,b)} = \frac{\partial}{\partial f_{(W,b)}}L'(W,b)\frac{\partial}{\partial W_i}f'_{(W,b)} \tag{8}$$

$$\frac{\partial}{\partial b_i}L_{(W,b)} = \frac{\partial}{\partial f_{(W,b)}}L'(W,b)\frac{\partial}{\partial b_i}f'_{(W,b)} \tag{9}$$

Among them, W_i, b_i are the weights and offsets that need to be updated, respectively, $L_{(W,b)}$ is the loss function, and $f_{(W,b)}$ is the input to the loss function. Then, in the next pass, we just need to replace $L_{(W,b)}$ with the current outer function and replace $f_{(W,b)}$ with the current outer outer function.

The weight update formula is:

$$W_o = W_i + \eta\frac{\partial}{\partial W}L_{(W,b)} \tag{10}$$

The offset update formula is:

$$b_o = b_i + \eta\frac{\partial}{\partial W}L_{(W,b)} \tag{11}$$

Among them, η is the current learning rate, and the learning rate can be adjusted according to the current training phase or the characteristics of the training set. W_i, b_i are the original weight and offset parameters respectively, and when updated, they become new weights W_o and offsets b_o.

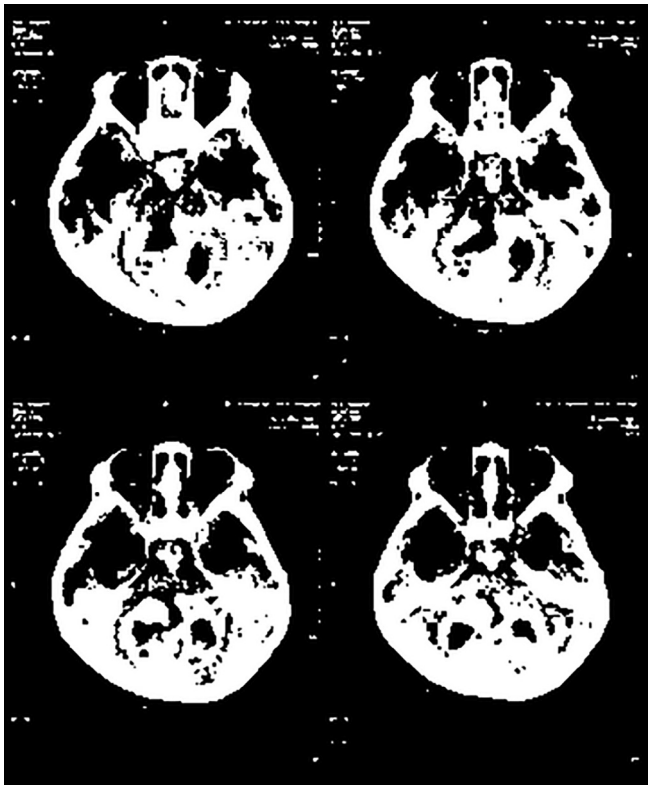

Fig. 8. Brain MRI image.

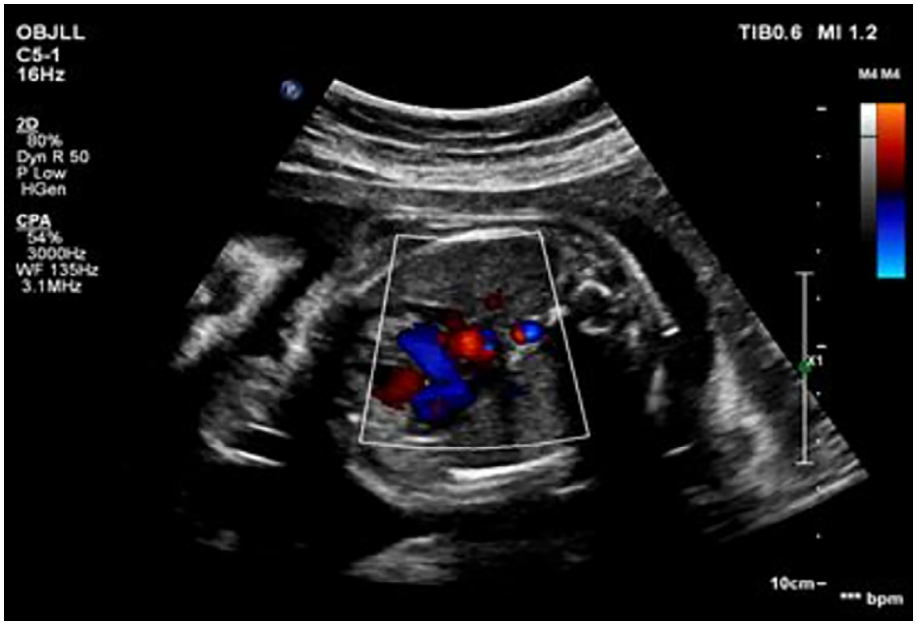

Fig. 9. Feature recognition of heart images.

3. Result

The patient opened the right upper extremity venous access and intravenously infused with compound sodium chloride injection. Moreover, under the local anesthesia, the left radial artery was placed and the pressure sensor was connected to monitor the brachial blood pressure. At the same time, the partial pressure of end-tidal carbon dioxide was maintained at 35–40 mmHg (1 mmHg = 0. 133 kPa). After anesthesia induction, the right internal jugular vein puncture was performed, and a three-chamber 7F central venous catheter (depth 13″–15 cm) was placed.

The primary pathway is used for intravenous blood delivery, one side is used to monitor central venous pressure, and the other side is used to pump vasoactive drugs. In the D1 group, 0.5 ug/kg dexmedetomidine (batch number: 1061034, Jiangsu Hengrui Pharmaceutical Co., Ltd.) was intravenously administered as a loading dose after induction of anesthesia. The injection was completed after 10 min, and then the patient was intravenously infused with O.5ll g/kedh until the surgery was completed. In the D2 group, the Dex1ug/kg load was intravenously injected after induction of anesthesia, and the intravenous infusion was continued for 0.5 g/kg/h to the end of surgery. Group C was intravenously infused with the same volume of normal saline at the same rate. Anesthesia maintenance: The patient inhaled 1%–2% sevoflurane, continued intravenous sufentanil 0.4 ~ O.7ug/kg/h, and the patient was injected intermittently with atracurium sulfonate to maintain muscle relaxation. During the CPB, sevoflurane was inhaled by artificial heart-lung machine to maintain anesthesia;

On the basis of this, the heart image of the infant and the image of the brain of the child are obtained, and the original cardiac MRI image obtained is shown in the following Fig. 7.

The detected brain image is as follows (Fig. 8).

In order to further study the characteristics of the above images, the algorithm proposed in this study is used for image processing to obtain the corresponding improved image, and the results are shown in the following Figs. 9 and 10.

4. Discussion and analysis

A significant increase in the concentration of catecholamines in the ischemic region of myocardial ischemia-reperfusion injury directly affects the myocardium. Moreover, inhibition of norepinephrine reuptake can lead to increased myocardial damage and loss of physiological myocardial protection mechanisms such

Fig. 10. Brain image feature recognition.

as ischemic preconditioning. Norepinephrine not only causes myocardial damage, but also increases blood endothelin levels, which is one of the important mediators of myocardial damage. After myocardial ischemia-reperfusion, the endothelin A (ETA) receptor is activated, which results in massive release of ET-1 and myocardial damage. Endothelin receptors are present in the sympathetic nerve endings of the heart, and sympathetic excitation causes a large release of endothelin, which causes damage to the myocardium. Q2 receptor agonists can reduce the stress response caused by surgical stimulation and inhibit the release of central catecholamine. Central sympathetic blockers can exert myocardial protection by affecting the Q2 receptor, and Q2 receptors are also present in sympathetic nerve endings. Presynaptic Q2 receptor excitation can reduce norepinephrine release. Dexmedetomidine is a selective receptor agonist that has central sedative and analgesic effects and reduces catecholamine levels in peripheral blood. In the myocardial ischemia-eperfusion injury, whether dexmedetomidine has an effect on endothelin-1 (ET-1) and norepinephrine has not been reported.

5. Conclusion

Based on the machine learning algorithm, this study combined with image processing to perform analysis and research that dexmedetomidine improves the anesthetic effect of infants with complex congenital heart surgery. Currently, anesthesia for pediatric surgery is generally performed under general anesthesia. The child has many troubles, discomfort, and separation from the parents before anesthesia. The intranasal administration of dexmedetomidine can solve this problem. In the pre-experiment of this study, the operation of tracheotomy and separation of the carotid, jugular, femoral, femoral veins was trained, and the floating catheter placement operation was successfully completed, which greatly reduced the physiological interference to the experimental animals, and greatly helped to reduce the mortality and improve the success rate of the experiment. At the same time, this paper collects the heart image of the infant and the original cardiac MRI image obtained from the brain image of the child, and uses the proposed algorithm to perform image processing, so as to obtain the corresponding improved image, and to adopt the proposed algorithm for image processing, and to obtain the corresponding improved image. From the research results, the method proposed in this study has certain validity.

6. Declarations

Xiaoyan Xu and Jianzhong Shuai designed the research framework and wrote the manuscript, and they equally contribute to this work.

Declaration of Competing Interest

The authors declare that they have no known competing financial interests or personal relationships that could have appeared to influence the work reported in this paper.

References

Ahmad, T., Sheikh, N.A., Akhter, N., et al., 2017. Intraoperative awareness and recall: a comparative study of dexmedetomidine and propofol in cardiac surgery. Cureus.

Alhammad, A.M., Baghdady, N.A., Mullin, R.A., et al., 2017. Evaluation of the impact of a prescribing guideline on the use of intraoperative dexmedetomidine at a tertiary academic medical center. Saudi Pharmaceut. J. 25 (1), 144–147.

Ama, E.H., Yassin, H.M., 2017. Effect of intranasal dexmedetomidine on emergence agitation after sevoflurane anesthesia in children undergoing tonsillectomy and/or adenoidectomy. Saudi J. Anaesthesia 11 (2), 137.

Amorim, Marco Aurélio, Soares, Govêia, Sousa, Catia, Magalhães, E., et al., 2017. Effect of dexmedetomidine in children undergoing general anesthesia with sevoflurane: a meta-analysis. Brazilian J. Anesthesiol. (English Ed.) 67 (2), 193–198.

Chen, X., Hu, J., Zhang, C., et al., 2018. Effect and mechanism of dexmedetomidine on lungs in patients of sepsis complicated with acute respiratory distress syndrome. Zhonghua Wei Zhong Bing Ji Jiu Yi Xue 30 (2), 151–155.

Frölich, M.A., Banks, C., Ness, T.J., 2017. The effect of sedation on cortical activation. Anesth. Analg. 124 (5), 1603–1610.

Hussain, N., Grzywacz, V.P., Ferreri, C.A., et al., 2017. Investigating the efficacy of dexmedetomidine as an adjuvant to local anesthesia in brachial plexus block: a systematic review and meta-analysis of 18 randomized controlled trials. Reg. Anesth. Pain Med. 42 (2), 184.

Jia, Z., Hao, H., Huang, M., et al., 2017. Influence of dexmedetomidine to cognitive function during recovery period for children with general anesthesia. Eur. Rev. Med. Pharmacol. Sci. 21 (5), 1106.

Jian-Xin, Z., Bing-Bing, L., Yan-Jun, L.I., et al., 2017. Effects of different doses of dexmedetomidine on inflammatory factors and T lymphocyte subsets in elderly patients undergoing laparoscopic surgery. J. Hainan Med. Univ. 23 (17).

Jo, Y.Y., Kim, J.Y., Lee, J.Y., et al., 2017. The effect of intraoperative dexmedetomidine on acute kidney injury after pediatric congenital heart surgery: a prospective randomized trial. Medicine 96, (28) e7480.

Khare, A., Sharma, S.P., Deganwa, M.L., et al., 2017. Effects of dexmedetomidine on intraoperative hemodynamics and propofol requirement in patients undergoing laparoscopic cholecystectomy. Anesthesia Essays Res. 11 (4), 1040–1045.

Küçükebe, Ö.B., Özzeybek, D., Abdullayev, R., et al., 2017. Effect of dexmedetomidine on acute lung injury in experimental ischemia-reperfusion model. Brazilian J. Anesthesiol. 67 (2), 139–146.

Li, Y., Liu, S., 2017. The effect of dexmedetomidine on oxidative stress response following cerebral ischemia-reperfusion in rats and the expression of intracellular adhesion molecule-1 (ICAM-1) and S100B. Med. Sci. Monit. 23, 867–873.

Makhni, R., Attri, J.P., Jain, P., et al., 2017. Comparison of dexmedetomidine and magnesium sulfate as adjuvants with ropivacaine for spinal anesthesia in infraumbilical surgeries and postoperative analgesia. Anesthesia Essays Res. 11 (1), 206–210.

Messeha, M.M., El-Morsy, G.Z., 2018. Comparison of intranasal dexmedetomidine compared to midazolam as a premedication in pediatrics with congenital heart disease undergoing cardiac catheterization. Anesthesia Essays Res. 12 (1), 170–175.

Miller, J.W., Ding, L., Gunter, J.B., et al., 2018. Comparison of intranasal dexmedetomidine and oral pentobarbital sedation for transthoracic echocardiography in infants and toddlers: a prospective, randomized, double-blind trial. Anesth. Analg. 126 (6), 1.

Mohamed, A., Mahmoud, S., Saad, M.O., et al., 2018. Effectivness of clonidine in treating dexmedetomidine withdrawal in a patient with co-existing psychiatric illness: a case report. Am. J. Case Rep. 19, 875–879.

Schäffer, Débora Passos Hinojosa, Otero, A.R., 2017. Cardiorespiratory effects of epidural anesthesia using lidocaine with morphine or dexmedetomidine in capuchin monkeys (Sapajus sp.) undergoing bilateral tubal ligation surgery, anesthetized with isoflurane. J. Med. Primatol. 46 (6).

Shen, J., Sun, Y., Han, D., et al., 2017. Effects of dexmedetomidine on perioperative cardiac adverse events in elderly patients with coronary heart disease. J. Central South Univ. 42 (5), 553.

Yoo, J.Y., Kwak, H.J., Kim, Y.B., et al., 2017. The effect of dexmedetomidine pretreatment on the median effective bolus dose of propofol for facilitating laryngeal mask airway insertion. J. Anesthesia 31 (1), 11–17.